Microbiology (2010), **156**, 313–326 DOI 10.1099/mic.0.035154-0

PAP1 [poly(A) polymerase 1] homozygosity and hyperadenylation are major determinants of increased mRNA stability of *CDR1* in azole-resistant clinical isolates of *Candida albicans*

Raman Manoharlal,[1] Jyotsna Gorantala,[2] Monika Sharma,[1] Dominique Sanglard[3] and Rajendra Prasad[1]

Correspondence
Rajendra Prasad
rp47@mail.jnu.ac.in *or*
rp47jnu@gmail.com

[1]Membrane Biology Laboratory, School of Life Sciences, Jawaharlal Nehru University, New Delhi, India

[2]School of Biotechnology, Jawaharlal Nehru University, New Delhi, India

[3]Institute of Microbiology, University Hospital Lausanne, Lausanne CH-1011, Switzerland

Received 2 October 2009
Revised 9 November 2009
Accepted 11 November 2009

Using genetically matched azole-susceptible (AS) and azole-resistant (AR) clinical isolates of *Candida albicans*, we recently demonstrated that *CDR1* overexpression in AR isolates is due to its enhanced transcriptional activation and mRNA stability. This study examines the molecular mechanisms underlying enhanced *CDR1* mRNA stability in AR isolates. Mapping of the 3′ untranslated region (3′ UTR) of *CDR1* revealed that it was rich in adenylate/uridylate (AU) elements, possessed heterogeneous polyadenylation sites, and had putative consensus sequences for RNA-binding proteins. Swapping of heterologous and chimeric *lacZ–CDR1* 3′ UTR transcriptional reporter fusion constructs did not alter the reporter activity in AS and AR isolates, indicating that *cis*-acting sequences within the *CDR1* 3′ UTR itself are not sufficient to confer the observed differential mRNA decay. Interestingly, the poly(A) tail of the *CDR1* mRNA of AR isolates was ~35–50 % hyperadenylated as compared with AS isolates. *C. albicans* poly(A) polymerase (*PAP1*), responsible for mRNA adenylation, resides on chromosome 5 in close proximity to the mating type-like (*MTL*) locus. Two different *PAP1* alleles, *PAP1-a*/*PAP1-*α, were recovered from AS (*MTL-a*/*MTL-*α), while a single type of *PAP1* allele (*PAP1-*α) was recovered from AR isolates (*MTL-*α/*MTL-*α). Among the heterozygous deletions of *PAP1-a* (Δ*pap1-a*/*PAP1-*α) and *PAP1-*α (*PAP1-a*/Δ*pap1-*α), only the former led to relatively enhanced drug resistance, to polyadenylation and to transcript stability of *CDR1* in the AS isolate. This suggests a dominant negative role of *PAP1-a* in *CDR1* transcript polyadenylation and stability. Taken together, our study provides the first evidence, to our knowledge, that loss of heterozygosity at the *PAP1* locus is linked to hyperadenylation and subsequent increased stability of *CDR1* transcripts, thus contributing to enhanced drug resistance.

INTRODUCTION

One of the major mechanisms of the multidrug resistance (MDR) phenotype in azole-resistant (AR) *Candida albicans* clinical isolates is characterized by the overexpression of genes encoding ATP binding cassette (ABC) multidrug transporters such as *CDR1/CDR2* (Akins, 2005; Prasad *et al.*, 1995; Sanglard *et al.*, 1995, 1997; Sanglard & Odds, 2002; White, 1997; White *et al.*, 1998), or major facilitator superfamily (MFS) pumps such as *CaMDR1* (Wirsching *et al.*, 2000). Once acquired, MDR is a stable phenotype that is maintained in AR clinical isolates even in the absence of selection pressure by the drugs (White, 1997; White *et al.*, 1997). This implies that some genetic alterations take place in the azole-susceptible (AS) isolates, resulting in constitutive overexpression of the drug efflux pump-encoding genes in AR isolates. Therefore, cellular elements contributing to the overexpression of MDR genes

Abbreviations: AR, azole-resistant; AS, azole-susceptible; LOH, loss of heterozygosity; MDR, multidrug resistance; Nou^R, nourseothricin-resistant; PAT, polyadenylation test; RACE, rapid amplification of cDNA ends; 3′ UTR, 3′ untranslated region.

A set of supplementary results, two supplementary figures and three supplementary tables, with references, are available with the online version of this paper. The supplementary results describe how 3′ UTR of *CDR1* mRNA forms altered secondary structures. The supplementary figures show the predicted secondary structure of *CDR1* 3′ UTR and the results of a *lacZ* mRNA decay assay. The supplementary tables list primers, plasmids and strains used in this study.

in AR isolates are very critical in designing strategies for therapeutic interventions.

Transcriptional regulation of *CDR1* has been extensively studied by several groups. It has been shown that *CDR1* harbours various consensus (Sp1, AP-1, Y-box) sequences as well as specific basal (BRE), negative (NRE) and drug/steroid response elements (DRE and SRE) in the 5′ flanking region (De Micheli *et al.*, 2002; Gaur *et al.*, 2004; Karnani *et al.*, 2004; Puri *et al.*, 1999). *Trans*-acting factors regulating *CDR1* have also been identified. For example, non dityrosine 80 (*CaNDT80*), a homologue of a meiosis specific transcription factor (TF) of *Saccharomyces cerevisiae*, has been identified as a potential activator of *CDR1* (Chen *et al.*, 2004). Coste *et al.* (2004) identified a TF, transcriptional activator of c*DR* genes (*TAC1*), that binds to the DRE in both the *CDR1* and the *CDR2* promoters. Interestingly, a TF belonging to the zinc cluster family, fluconazole resistance 1 (*FCR1*) (Talibi & Raymond, 1999), as well as the global repressor thymidine uptake 1 (*Tup1*), acts as a negative regulator of *CDR1* expression (Yang *et al.*, 2006). Recent genome-wide location profiling (ChIP-chip) results show that another TF of the zinc cluster family, uptake control 2 (*Upc2*), which regulates *ERG* genes, also targets *CDR1* (Znaidi *et al.*, 2008). The efforts of several groups have also led to the identification of various *cis*-acting elements such as the H_2O_2 responsive element (HRE) and the benomyl responsive element (BRE) in the *MDR1* promoter region, mediating its upregulation in AS isolates and its constitutive activation in AR isolates (Rognon *et al.*, 2006). Recently a zinc cluster TF, designated multidrug resistance regulator 1 (*MRR1*), has been identified, which is linked to the activation of *MDR1* expression. Inactivation of *MRR1* abolishes the resistance of Mdr1p-overexpressing strains (Morschhäuser *et al.*, 2007).

It is thus apparent that transcriptional regulation plays an important role in the mechanism underlying the overexpression of MDR genes; however, the relevance of the post-transcriptional events associated with it is poorly understood. By employing two pairs of matched *C. albicans* clinical isolates in which azole resistance developed due to the overexpression of *CDR1* during prolonged azole therapy, we have recently shown that the high mRNA levels in AR isolates are predominantly contributed by both enhanced transcriptional activation and mRNA stability (Manoharlal *et al.*, 2008). In this study, we further dissected the molecular basis of *CDR1* mRNA turnover in matched clinical isolates. For this, we have identified and characterized the complete 3′ end of the *CDR1* mRNA by the 3′-rapid amplification of cDNA ends (3′-RACE)-PCR method in these matched isolates. Our observations with chimeric *lacZ–CDR1* 3′ UTR transcriptional reporter fusion transformants ruled out the participation of the 3′ UTR in transcriptional as well as post-transcriptional control of *CDR1*. However, there was an increase in poly(A) tail length, which coincided with the enhanced *CDR1* mRNA stability in AR isolates. Poly(A) tail synthesis in *C. albicans* is catalysed by the nuclear poly(A) polymerase that resides within the mating type-like (*MTL*) locus on chromosome 5.

The *MTL* loci of *C. albicans* span approximately 9 kb and contain *S. cerevisiae* mating-type homologues *MAT-a1*, *MAT-α1* and *MAT-α2* (Hull & Johnson, 1999), as well as genes unique to fungal mating loci, including *OBP* (an oxysterol-binding protein), *PAP1* [a poly(A) polymerase 1] and *PIK1* (a phosphoinositol kinase). A copy of each of these three genes is present in both the *MTL-a* and the *MTL-α* locus. The *MTL* genes have no significant homology to each other. The *a* and *α* versions of *PAP1*, *PIK1* and *OBP* have approximately 60 % homology to each other. Most wild-type *C. albicans* strains are diploid and have both the *MTL-a* and *MTL-α* loci (Magee & Magee, 2000). However, our analysis of *PAP1* allelic status revealed that *MTL* heterozygosity (*MTL-a/MTL-α*) and homozygosity (*MTL-α/MTL-α*) are linked to the acquisition of *PAP1* heterozygosity (*PAP1-a/PAP1-α*) and homozygosity (*PAP1-α/PAP1-α*) in AS and AR isolates, respectively. We also show that heterozygous disruption of *PAP1-a* conferred relatively enhanced drug resistance, hyperadenylation and increased stability of *CDR1* transcripts in AS isolates. However, heterozygous disruption of *PAP1-α* in AS and AR affected neither the drug resistance nor the polyadenylation or stability of *CDR1* transcripts. Therefore, our results provide evidence that loss of heterozygosity (LOH) at the *PAP1* locus is associated with the hyperadenylation and increased stability of *CDR1* transcripts and that this helps the development of drug resistance in AR isolates.

METHODS

Materials. Media chemicals were obtained from HiMedia. Luria–Bertani broth and agar media were purchased from Difco, BD Biosciences. Restriction endonucleases, DNA-modifying enzymes, *Taq* DNA polymerase and ultrapure deoxyribonucleotides (dATP, dGTP, dCTP and dTTP) for PCR were purchased from New England Biolabs. Moloney murine leukaemia virus (M-MuLV) reverse transcriptase, IPTG, X-Gal, T7 and Sp6 promoter primers were obtained from MBI Fermentas. Radiolabelled [α-^{32}P]dATP was obtained from Bhabha Atomic Research Center (BARC), India. The Megaprime DNA labelling system was procured from Amersham Pharmacia Biotech. The pGEMT-Easy vector system II used for T/A DNA cloning purposes was purchased from Promega. Nourseothricin was obtained from Werner Bioagents. Gel elution and PCR purification kits were obtained from Qiagen. Oligonucleotides used were commercially synthesized by Sigma–Aldrich (Supplementary Table S1). All molecular biology grade chemicals used in this study were obtained from Sigma Chemical.

Bacterial and yeast strains and growth media. *Escherichia coli* DH-5α was used as a host for plasmid construction and propagation. Plasmids and *C. albicans* strains used in this study are listed in Supplementary Tables S2 and S3. *E. coli* was cultured in Luria–Bertani broth media to which ampicillin was added (100 μg ml^{-1}). *C. albicans* strains were maintained on yeast extract peptone dextrose (YEPD) media. For agar plates, 2.5 % (w/v) Bacto Agar was added to the medium. All strains were stored as frozen stocks with 15 % (v/v)

glycerol at −80 °C. Before each experiment, cells were freshly revived on YEPD plates from this stock.

3′-Rapid amplification of cDNA ends (3′-RACE). The nucleotide sequence of the oligonucleotide primers used for the reverse transcription-3′-RACE-nested PCR were selected based on the published sequences of *CDR1* (GenBank accession no. X77589) (Prasad *et al.*, 1995). Total RNA isolated from each isolate using the TRIzol reagent (as per the manufacturer's specifications) was enriched with poly(A)$^+$ (polyadenylated) mRNA using the Oligotex mRNA Mini kit protocol (Qiagen) and used subsequently for performing the reverse transcription-3′-RACE reaction as described elsewhere (Gerads & Ernst, 1998). For a typical 3′-RACE reaction, cDNA synthesized from ~0.1 μg poly(A)$^+$ RNA was placed in a 0.5 ml reaction tube with 1 μM oligo(dT)$_{18}$ anchor primer stock, and the volume was adjusted to 11 μl with diethylpyrocarbonate (DEPC)-treated water (Fig. 1a, step 1). The mixture was incubated for 10 min at 70 °C and chilled on ice for 1 min, after which the remainder of the reaction mixture was added from a master mix to the reaction tube in order for each reaction to contain a 1 mM concentration of each of dATP, dCTP, dGTP and dTTP, and 40 U RNase inhibitor (MBI, Fermentas) in a buffer consisting of 50 mM Tris/HCl (pH 8.3), 50 mM KCl, 4 mM $MgCl_2$ and 10 mM DTT. After brief mixing, the reaction was incubated for 10 min at 37 °C followed by addition of

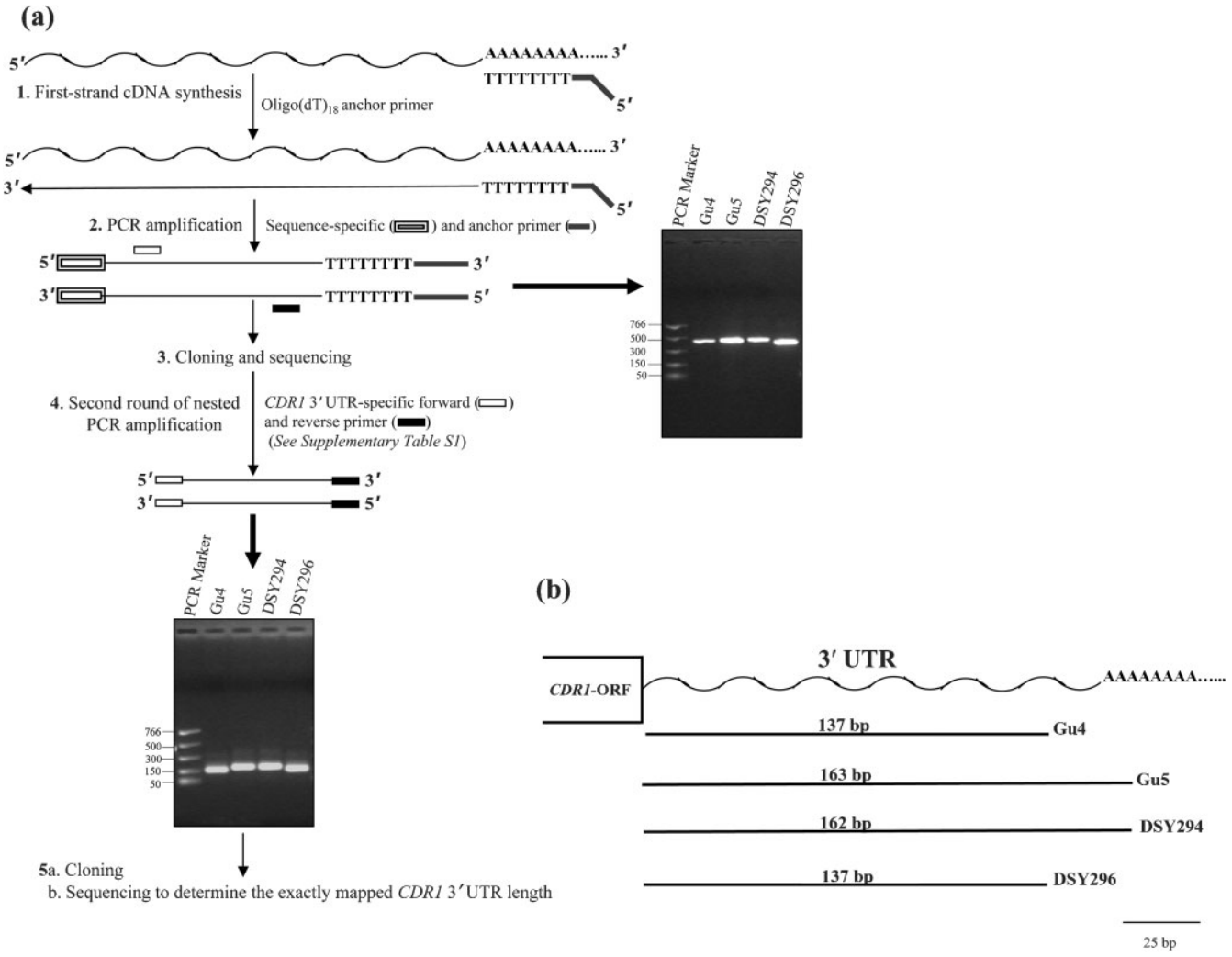

Fig. 1. Determination of termination sites of *CDR1* mRNA. (a) The 3′-RACE strategy employed for the detection of *CDR1* 3′ UTR length is detailed in Methods. Briefly, cDNA synthesized from poly(A)$^+$-enriched mRNA samples from clinical *C. albicans* isolates was PCR-amplified using *CDR1*-specific forward and reverse anchor primers. Following electrophoresis, the amplified PCR products were visualized by staining with ethidium bromide (indicated by a long thick arrow), cloned and sequenced. To confirm the RT-PCR specificity, another round of 3′ UTR-specific nested PCR amplification of *CDR1* of each isolate was performed. Following electrophoresis, the amplified PCR products were further visualized by staining with ethidium bromide (indicated by a short thick arrow), cloned and sequenced. The locations of DNA size markers (bp) are marked on the left-hand side of the gel. *C. albicans* isolates are labelled above the gels. (b) Schematic representations of the mapped 3′ UTRs of *CDR1*. The open box and wavy line represent the *CDR1*-coding and poly(A) tail-harbouring 3′ end regions respectively, while thick straight lines with numbers on top indicate the mapped *CDR1* 3′ UTR length of each isolate.

40 U M-MuLV reverse transcriptase (MBI, Fermentas). Finally, the reaction was incubated at 37 °C for 60 min and then stopped by heating at 70 °C for 10 min followed by chilling on ice for 1 min. The synthesized cDNA was used for amplification of the *CDR1* mRNA-specific 3′ end of each isolate (Fig. 1a, step 2), using the corresponding appropriate dilution of cDNA as template (determined empirically for *CDR1* to give a product in the linear range, generally 1 : 4) and 1 μM of each *CDR1*-specific forward primer CT-*CDR1*-F-RM (corresponding to positions 4271–4293 in the *CDR1* genomic sequence) and reverse PCR anchor primer as described in Supplementary Table S1. PCR parameters were initial denaturation of 95 °C for 5 min, followed by 35 cycles of denaturation at 95 °C for 30 s, annealing at 55 °C for 40 s, elongation at 72 °C for 40 s and final extension at 72 °C for 10 min. As a positive control, *CDR1*-specific forward primer CT-*CDR1*-F-RM and reverse primer CT-*CDR1*-R-RM (corresponding to positions 4475–4503 in the *CDR1* genomic sequence) were also used (data not shown). The negative control (without reverse transcriptase) established that the PCR products generated in the RT-PCR were not due to genomic DNA contamination (data not shown). The RT-PCR product of each isolate was electrophoresed on a 1.2 % agarose gel in 1 × TAE. The gel-purified 3′-RACE product (Qiagen PCR Cleanup kit) of each isolate was cloned directly in the pGEMT-Easy vector using a T/A cloning kit (Promega) as per the manufacturer's recommendations and sequenced (Fig. 1a, step 3). The corresponding clone of each isolate was sequenced and subsequently used as template for a second nested PCR amplification of *CDR1* (Fig. 1a, step 4) with forward and reverse primers (UTR-F-*Pac*I and UTR-R-*Mlu*I, Supplementary Table S1) specific to each isolate. PCR parameters were: initial denaturation at 95 °C, followed by 30 cycles of denaturation at 95 °C for 30 s, annealing at 55 °C for 30 s, elongation at 72 °C for 30 s and final extension at 72 °C for 10 min. The resulting PCR-amplified fragments (now exactly specific to mapped 3′ UTR *CDR1* of each isolate) were purified (Qiagen PCR Cleanup kit) and further subcloned in pGEMT-Easy (Fig. 1a, step 5a), generating *CDR1* 3′ UTR-specific clones of each isolate, as described in Supplementary Table S2. All the cloned PCR-amplified products were confirmed by appropriate restriction digestion analysis and sequenced further to determine the exact and precise length of the *CDR1* 3′ UTR (Fig. 1a, step 5b).

Custom service nucleotide sequencing. Multiple 3′ UTR-specific clones of each isolate were sequenced directly by extension from both sense and antisense strands using T7 promoter/T7 promoter primer and SP6 promoter/SP6 promoter primer (Supplementary Table S1) by exploiting BigDye Terminator chemistry and an automated DNA sequencer (ABI Prism 3100). Reproducibility of the sequencing was confirmed by processing all samples at least twice.

Sequence alignments, *in silico* analysis and computerized secondary structure predictions of *CDR1* 3′ UTR. Multiple sequence alignment of mapped *CDR1* 3′ UTR for both matched pairs of isolates was done using the CLUSTAL W (version 1.83) program (Thompson *et al.*, 1994). *In silico* analysis of the 3′ UTR for prediction of the putative regulatory site was carried out by the UTRscan (UTResources) program (Pesole *et al.*, 2002; Pesole & Liuni, 1999). We used the mfold (version 3.0) algorithm created by Zuker *et al.* (1999) for *in silico* computer predictions of the secondary structure of the 3′ UTR by a minimization of free energy-based method. The folding temperature was fixed at 37 °C and ionic conditions were 1 M NaCl without constraints, and no limit in the maximum distance between paired bases.

Reporter plasmid construction. Plasmid pCPL51 (Manoharlal *et al.*, 2008), harbouring P_{CDR1}–*lacZ*, was used for cloning of the mapped *CDR1* 3′ UTR in transcriptional fusion with a heterologous *lacZ* reporter. For this purpose, sequences at the junctions of *lacZ*–T_{ACT1} and T_{ACT1}–*caSAT1* were mutated sequentially by introducing *Pac*I and *Mlu*I sites at these corresponding junctions (*lacZ*–T_{ACT1} and T_{ACT1}–*CaSAT1*) using *lacZ*-F-*Pac*I-RM/*lacZ*-R-*Pac*I-RM and *lacZ*-F-*Mlu*I-RM/*lacZ*-R-*Mlu*I-RM primers (Supplementary Table S1) with a QuikChange site-directed mutagenesis system (Stratagene) to generate the plasmids pCPL53-RM (with *Pac*I site only) and pCPL54-RM (with both *Pac*I and *Mlu*I sites introduced), respectively. Mapped *CDR1* 3′ UTR fragments of each isolate were excised from their corresponding 3′ UTR-harbouring pGEMT-Easy vector clones (Supplementary Table S2) by digestion at *Pac*I and *Mlu*I sites (sites introduced in primers during the synthesis), and further subcloned in *Pac*I/*Mlu*I-digested pCPL54-RM to generate pCPL54-Gu4/Gu5-3′UTR-RM and pCPL54-DSY294/DSY296-3′UTR-RM (Supplementary Table S2). All constructs were confirmed by appropriate restriction digestion analysis. The flanking *CDR1* sequences in all these plasmids served for genomic integration of the P_{CDR1}-*lacZ*-3′ UTR reporter fusion cassettes at the native *CDR1* locus, and the dominant *CaSAT1* marker (Reuss *et al.*, 2004) was used to select nourseothricin-resistant (Nou^R) transformants.

Yeast transformation. *C. albicans* was transformed by the standard electroporation protocol (Reuss *et al.*, 2004). Briefly, 5 μl (~1 μg) of the specific enzyme-digested and gel-purified linearized DNA fragments was mixed with 40 μl electrocompetent cells and electroporated using a Bio-Rad Genepulser XL (0.2 cm cuvette, 1.5 kV). Following electroporation, transformants were washed with 1 ml 1 M sorbitol, resuspended in 1 ml YEPD medium and incubated for 3–4 h with shaking at 30 °C prior to plating on YEPD plates containing 200 μg nourseothricin ml^{-1} and grown at 30 °C. Nou^R transformants were picked after 1 day of growth and restreaked on YEPD plates containing 100 μg nourseothricin ml^{-1}.

β-Galactosidase reporter assay. β-Galactosidase assays were performed using duplicate samples of cells from three independent experiments, as described by Uhl & Johnson (2001). β-Galactosidase activity was determined by the standard equation and expressed in Miller units (mg protein)$^{-1}$. Miller units are arbitrary units:

$$\beta\text{-Galactosidase activity (Miller units)} = (A_{420} \times 1000)/(OD_{600} \times t \times v)$$

where t is the time of reaction (min) and v is the culture volume (ml).

Polyadenylation test (PAT) analysis of poly(A) tail length. A new and improved variation of the 3′-RACE PAT involving G-tailing of mRNA was employed to show both the presence of the poly(A) tail and its length, as described elsewhere (Kusov *et al.*, 2001).

Guanylation of mRNA. The purified poly(A)$^+$-enriched mRNA (as described above) was used directly for polyguanylation using yeast poly(A) polymerase (PAP) (catalogue number E74225Y, Amersham Pharmacia Biotech/US Biochemicals) as per the manufacturer's recommendations. To abolish the higher-ordered secondary structure at the 3′ end of the mRNA, samples (0.1 μg) were heated at 65 °C for 5 min and immediately placed on ice. They were incubated for 1 h at 37 °C with 600 U PAP and 0.5 mM GTP in a 25 μl reaction mixture containing 20 mM Tris/HCl (pH 7.0), 50 mM KCl, 0.7 mM $MnCl_2$, 0.2 mM EDTA, 100 μg BSA ml^{-1} and 10 % (v/v) glycerol. An additional 300 U PAP was further added and incubation was continued for an additional 1 h. The reaction was terminated by heat treatment at 65 °C for 10 min, chilled on ice and kept at −80 °C till further use.

RT-PCR. Polyguanylated mRNA (as described above) was subjected directly to RT-PCR analysis using hot start conditions (65 °C, 30 s). The first-strand cDNA synthesis (reverse-transcription, 42 °C for 1 h) was primed by oligo(dC_9T_6)-anchor primer (1 μM). The reverse-transcription reaction was stopped by denaturation at 70 °C for 10 min; the synthesized cDNA product (1 : 4 dilution) was used for

PCR amplification with 1 μM of each *CDR1*-specific forward primer (CT-*CDR1*-F/UTR-F-*Pac*I) and reverse anchor primer as described in Supplementary Table S1. PCR parameters were: initial denaturation of 95 °C for 5 min, followed by 35 cycles of denaturation at 95 °C for 30 s, annealing at 55 °C for 30 s, elongation at 72 °C for 1 min and final extension at 72 °C for 10 min. The PCR products were gel-purified and used for cloning into the T/A cloning vector as recommended by the manufacturer (Promega). Approximately 8–10 random clones from at least three independent RT-PCRs for each isolate were sequenced.

Construction of gene disruption cassettes. Two different *PAP1* disruption cassettes were designed in this study. Two cassettes, *C1* and *C2*, in plasmids pRM3 and pRM4 were designed using the *URA*-blaster system (Fonzi & Irwin, 1993). *C1* bears the deletion of a portion of 602 bp between nucleotides +500 and +1102 with respect to the first ATG codon of *PAP1-a*. *C2* was designed to delete a region of 636 bp between nucleotides +750 and +1386 with respect to the first ATG codon. To construct these two deletion cassettes (*C1* and *C2*), the entire *PAP1-a* ORF and a portion of the *PAP1-α* ORF (corresponding to nucleotides +259 to +1677 with respect to the first ATG codon) were first amplified from genomic DNA of DSY294 and DSY296, respectively, using the cloning primer pairs PAP-a-F-*Bam*HI-RM/PAP-a-R-*Xho*I-RM and PAP-alpha-F-*Bam*HI-RM/PAP-alpha-R-*Xho*I-RM, respectively (Supplementary Table S1). The resulting PCR fragments were cloned into pBluescript-KS(+) to yield pRM1 and pRM2, respectively (Supplementary Table S2). For disruption with cassettes *C1* and *C2*, deletions were created from pRM1 and pRM2 by PCR using deletion primer pairs PAP-a-F-*Bgl*II-RM/PAP-a-R-*Pst*I-RM and PAP-alpha-F-*Bgl*II-RM/PAP-alpha-R-*Pst*I-RM, respectively (Supplementary Table S1). The obtained PCR fragment was digested with *Pst*I and *Bgl*II, and the 3.7 kb *Pst*I/*Bgl*II *URA3*-blaster fragment from pMB7 (Fonzi & Irwin, 1993) was inserted to obtain deletion constructs pRM3 and pRM4, respectively (Supplementary Table S2). The linearized fragments *C1* and *C2*, obtained by digestion of deletion constructs (pRM3 and pRM4) with *Apa*I/*Sac*I, were used for transformation in *C. albicans*. It is of note that Δ*ura3* mutants of the clinical isolates DSY294 and DSY296, i.e. DSY3040 and DSY3041 (Coste *et al.*, 2006), respectively, were used for *PAP1* disruptions and subsequent experiments. After generation of heterozygous mutants for each allele, the *ura3* marker was regenerated by plating Ura^+ colonies on selective medium containing 5-fluoroorotic acid (5-FOA), as described previously (Sanglard *et al.*, 1996). The verification of heterozygous mutants was performed by PCR using an internal and an external recombination-specific primer (results not shown).

Construction of revertant strains. Complementation of heterozygous *PAP1* mutants was achieved by expression of *PAP1-a* and *PAP1-α* under the control of their native promoters. *PAP1-a* and *PAP1-α* ORFs with 500 bp of the 5′- and 3′-flanking regions were amplified from genomic DNA of DSY294 and DSY296, respectively, by PCR with primer pairs PAP-aC-F-*Xho*I-RM/PAP-aC-R-*Pst*I-RM and PAP-alphaC-F-*Xho*I-RM/PAP-alphaC-R-*Pst*I-RM, respectively (Supplementary Table S1). The resulting PCR fragment was digested with restriction enzymes *Xho*I and *Pst*I (sites introduced in primers during the synthesis) and cloned in the same sites of the CIp10 vector (Murad *et al.*, 2000) to yield pRM5 (harbouring *PAP1-a*) and pRM6 (harbouring *PAP1-α*). CIp10-derived plasmids pRM5 and pRM6, harbouring nourseothricin as selectable marker, were digested with *Stu*I and used to transform heterozygous *PAP1* mutants in which the *ura3* marker had been regenerated as described above (Supplementary Table S3). The Nou^R transformants were analysed by PCR to confirm the reintegration of the *PAP1* alleles.

Drug susceptibility testing. Drug susceptibility testing was performed by spotting cells onto solid agar plates containing the tested drugs (see Fig. 5 for drug concentrations used). Yeast cultures were grown overnight in YEPD and diluted to a density of 1.5×10^7 cells ml^{-1}, and 10-fold serial dilutions were performed to a final dilution step containing 1.5×10^3 cells ml^{-1}. Five microlitres of each dilution were spotted onto YEPD plates with or without drugs. Plates were incubated for 48 h at 30 °C.

Thiolutin chase assay. To measure the *CDR1* mRNA half-life, a potent *in vivo* transcriptional inhibitor of *C. albicans*, thiolutin, at an optimized concentration (40 μg) was used as described previously (Manoharlal *et al.*, 2008). Briefly, 100 ml cells was grown at 30 °C to OD_{600} 1.0. Aliquots of cells were taken at the indicated times after transcriptional shutoff by thiolutin. Total RNA was isolated using the Ambion RiboPure-Yeast RNA isolation kit (catalogue no. 1926) as per the manufacturer's instructions. Equal RNA loading was assessed by staining the agarose gel with ethidium bromide prior to blotting. For Northern blots, ~25 μg total RNA from the above samples was hybridized with a single probe derived from *CDR1*-specific primers (primer pairs KM1 and KM2, Supplementary Table S1) that was used throughout this study. Hybridization signal intensity was quantified with a phosphorimager scanner (FLA-5000, FLA5000 Fuji phosphorimager), normalized to the band intensity at time t_0 and plotted as a line graph.

RESULTS

We have analysed two pairs of matched clinical AS and AR *C. albicans* strains isolated from recurrent episodes of oropharyngeal candidiasis (OPC) in two different human immunodeficiency virus-positive (HIV^+) AIDS patients, in whom MDR in AR isolates is predominantly linked to overexpression of *CDR1* (Franz *et al.*, 1999; Sanglard *et al.*, 1995). Our recent study on the molecular characterization of *CDR1* and its products (mRNA/protein) in these clinical isolates suggested that the MDR phenotype is governed by enhanced transcription activation and the mRNA stability of the *CDR1* transcript (Manoharlal *et al.*, 2008). In this study, we have explored the molecular basis of the mRNA stability of *CDR1* in AR isolates.

The 3′ UTR of *CDR1* mRNA displays length heterogeneity

As an initial step to study the post-transcriptional mechanisms involved in enhanced *CDR1* mRNA stability, transcription termination sites of *CDR1* in AS and AR isolates were determined by the 3′-RACE method (Gerads & Ernst, 1998). For this, RT-PCR products of *CDR1* of each isolate were generated (Fig. 1a, step 1 and 2) using the *CDR1*-specific forward primer CT-*CDR1*-F-RM and oligo$(dT)_{18}$AP-RM anchor primer (Supplementary Table S1), cloned directly into the pGEMT-Easy vector and sequenced (Fig. 1a, step 3). To further confirm the RT-PCR specificity of *CDR1* (because of close homology of *CDR1* with *CDR2*), a subsequent second round of nested PCR of corresponding *CDR1* 3′ UTR-harbouring clones (Fig. 1a, step 3) was performed with *CDR1* 3′ UTR-specific primers for each isolate (Fig. 1a, step 4) (Supplementary Table S1). 3′ UTR products specific to *CDR1* for each isolate were amplified and further subcloned into pGEMT-Easy (Fig. 1a, step 5a). Direct sequencing (Fig. 1a, step 5b) of multiple

3′ UTR-specific clones of AS and AR isolates confirmed and revealed exact transcription termination sites of *CDR1* (data not shown). For the matched isolates Gu4/Gu5 and DSY294/DSY296, 3′ UTR length was mapped to 137/163 bases and 162/137 bases, respectively (positions are relative to the UAA stop codon) (Fig. 1b).

CDR1 3′ UTR sequences reveal polymorphism and potential mRNA destabilizing signals

Since differences in sequence at the 3′ UTR could be involved in polyadenylation site selection (Edwalds-Gilbert *et al.*, 1997) and mRNA stability (Russell *et al.*, 1998), we did a comparative *in silico* analysis of mapped 3′ UTR fragments of *CDR1* of AS and AR isolates and analysed their relevant sequence features. 3′ UTR sequence alignment of *CDR1* revealed polymorphism at positions −7U (insertion), U19C and C64U (substitution) [Fig. 2a, open box, where the base(s) before and after the number is the sequence from Gu4 and Gu5 isolates, respectively] and an additional extended 26 and 25 base AU (adenylate/uridylate)-rich stretch at the 3′ end for only Gu5 (AR) and DSY294 (AS) isolates, respectively (Fig. 2a). All nucleotide positions are relative to the UAA translational stop codon (considered as +1).

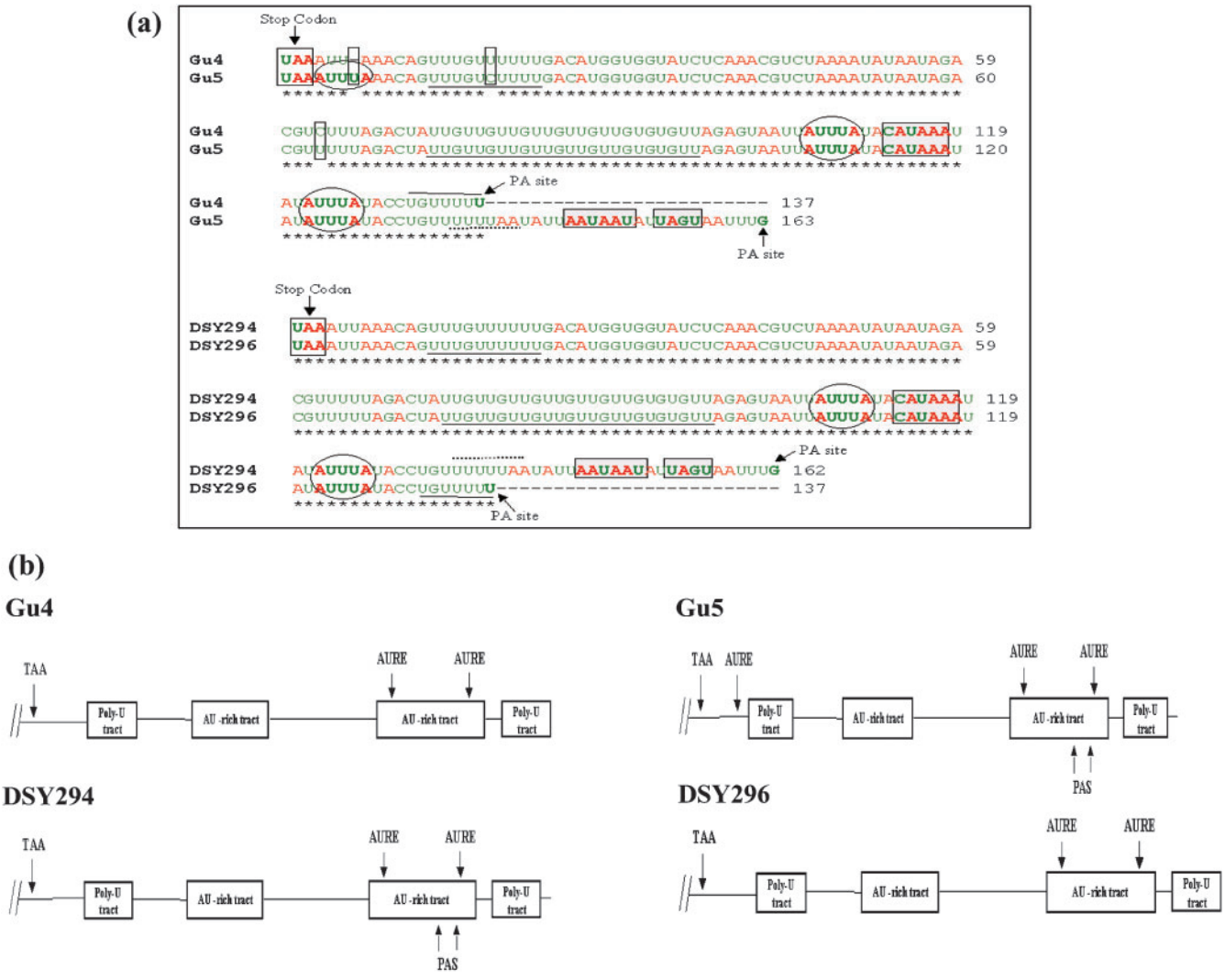

Fig. 2. Sequence analysis of *CDR1* 3′ UTR. (a) Alignment of *CDR1* 3′ UTRs from the two matched pairs of clinical isolates obtained using the CLUSTAL W program (Thompson *et al.*, 1994). Conserved residues are indicated by asterisks. Mismatched residues are represented by open boxes. Gaps (marked with dashes) have been introduced to maximize the alignments. Continuous and discontinuous underlining denotes the polypyrimidine (Py) and cytoplasmic polyadenylation element (CPE) tract, respectively. The eukaryotic poly(A) signal is indicated by shaded boxes. Elliptical boxes denote the AU-rich elements (AAUAAA). Numbers at the right are relative to the UAA translational stop codon (considered as position +1). (b) Schematic representation of the predicted regulatory motifs in the 3′ UTR, indicated by boxes.

The *CDR1* 3′ UTR is ~78 % AU, represents several putative consensus sequences for cytoplasmic RNA-binding protein(s) (Fig. 2b), and has perfect AU-rich elements (AURE) (Fig. 2a, elliptical boxes). The AURE motifs are characterized by the presence of the consensus sequence (AUUUA) and have been reported to be involved in destabilization of their corresponding mRNAs (Trzaska & Dastych, 2005). The presence of one perfect (UAGU) and two degenerate (A/CAUAAA, AAUAAA/U) yeast polyadenylation signals (Fig. 2a, shaded boxes), suggests that mRNA variants influence the *CDR1* mRNA steady-state levels, as has been reported for other cells (Edwalds-Gilbert *et al.*, 1997; Higgins, 1991; Hsu *et al.*, 1990). A poly(U)-rich and a cytoplasmic polyadenylation element (CPE) tract were also predicted (Fig. 2a, continuous and discontinuous underlining, respectively).

3′ UTR swapping does not affect β-galactosidase reporter activity

The sequence and structure analyses of the 3′ UTR of *CDR1* suggested that the polymorphism (Fig. 2a) as well as differential secondary structure (Supplementary Fig. S1) of AS and AR isolates contribute to the observed enhanced mRNA stability. To obtain direct experimental evidence, we tested whether the *CDR1* 3′ UTR from AS isolates has any mRNA destabilizing effect in AR isolates and vice versa. For this purpose, expression vectors harbouring P_{CDR1}-*lacZ*-*CDR1* 3′ UTR chimeric transcriptional reporter fusions were constructed (Fig. 3a, see Methods). The linearized transformation cassette of each isolate was integrated into the native *CDR1* genomic locus in corresponding matched isolates. Single-copy integration of each construct was confirmed by Southern hybridization (data not shown). Two representative Nou^R transformants of each parental strain were used for further analysis. The resulting reporter strains were designated Gu4L2-CUN (P_{CDR1}-*lacZ*-3′UTR^N), Gu4L2-CUS (P_{CDR1}-*lacZ*-3′UTR^S); Gu5L2-CUN (P_{CDR1}-*lacZ*-3′UTR^N), Gu5L2-CUS (P_{CDR1}-*lacZ*-3′UTR^S); DSY294L2-CUN (P_{CDR1}-*lacZ*-3′UTR^N), DSY294L2-CUS (P_{CDR1}-*lacZ*-3′UTR^S); and DSY296L2-CUN (P_{CDR1}-*lacZ*-3′UTR^N) and DSY296L2-CUS (P_{CDR1}-*lacZ*-3′UTR^S). The superscripts 'N' and 'S' in the designated constructs stand for native and swapped *CDR1* 3′ UTR reporter transformants, respectively.

Expression of the *lacZ* reporter gene in various strains was qualitatively assessed by comparing the intensity of the blue colour produced by cells grown on agar plates containing the indicator dye X-Gal (Fig. 3b), and was quantified by measuring the β-galactosidase reporter activity in liquid assays (Fig. 3c). Two observations emerged from these results. First, the β-galactosidase activity observed in native as well as swapped 3′ UTR transformants of each AR isolate was always higher than their corresponding AS reporter transformants (3.22-fold for Gu5L2-CUN versus Gu4L2-CUN, 2.33-fold for Gu5L2-CUS versus Gu4L2-CUS; 4.44-fold for DSY296L2-CUN versus DSY294L2-CUN and 3.86-fold for DSY296L2-CUS versus DSY294L2-CUS). Second, the reporter activity of the 3′ UTR native transformants of either AS or AR isolates was comparable with that of their corresponding swapped reporter fusion transformants (Gu4L2-CUN versus Gu4L2-CUS, Gu5L2-CUN versus Gu5L2-CUS, DSY294L2-CUN versus DSY294L2-CUS, and DSY296L2-CUN versus DSY294L2-CUS). Thus, swapping of the *CDR1* 3′ UTR of AS and AR isolates did not affect the reporter activity. In another set of experiments, we observed comparable *lacZ* transcript half-lives in native as well as swapped 3′ UTRs of *CDR1* in both AS and AR isolates (Supplementary Fig. S2). The influence of the 3′ UTR of *CDR1* was measured by employing a heterologous *lacZ* reporter. However, the possibility that the *CDR1* 3′ UTR might have a *cis* effect on transcriptional or post-transcriptional control of its transcript cannot be ruled out.

CDR1 mRNA poly(A) tail length is longer in AR isolates

Since poly(A) tail removal is a critical step in the 3′-exonuclease-mediated mRNA decay pathway (Higgins, 1991; McCarthy, 1998; Ross, 1996), we checked the polyadenylation status of *CDR1* mRNA between AS and AR isolates. For this, we employed a recently described PCR-based PAT assay, where the 3′ end of the mRNA is polyguanylated using yeast poly(A) polymerase, as described earlier (Kusov *et al.*, 2001). With this step, a poly(A)–oligo(G) junction is generated, which serves as specific target for the amplification of the 3′ end of the transcriptome with the universal reverse oligo(dC_9T_6) anchor primer and a gene-specific forward primer. RT-PCR products were cloned and sequenced for the accurate measurement of poly(A) tail length. Chromatogram analysis of cloned PAT-PCR products of each AS and AR isolate confirmed precisely that the *CDR1* poly(A) tail length was shorter, with 24 ± 2 A residues in AS isolates, in contrast to 35 ± 2 A residues in AR isolates (Table 1; a maximum variation of ± 2 bases was observed between different clones). It should be mentioned that a minimum of 10 random clones were subjected to sequencing to determine the precise poly(A) tail length.

Poly(A) polymerase 1 (*PAP1*) is heterozygous (*PAP1-a/PAP1-α*) in AS isolates but homozygous (*PAP1-α/PAP1-α*) in AR isolates

In eukaryotes, poly(A) tail synthesis at the 3′ end of mRNAs in the nucleus is catalysed by the canonical poly(A) polymerase (*PAP*), which belongs to the DNA polymerase-like nucleotidyl transferase superfamily (Holm & Sander, 1995). *C. albicans* poly(A) polymerase (*PAP1*) is located within the *MTL* locus on chromosome 5 (Coste *et al.*, 2006). To analyse the *PAP1* allelic status in AS and AR isolates, oligonucleotides were designed to specifically amplify the two *PAP1* alleles *PAP1-a* and *PAP1-α* (Supplementary Table S1). For this, multiplex PCR was performed with genomic DNA of each of the isolates, as

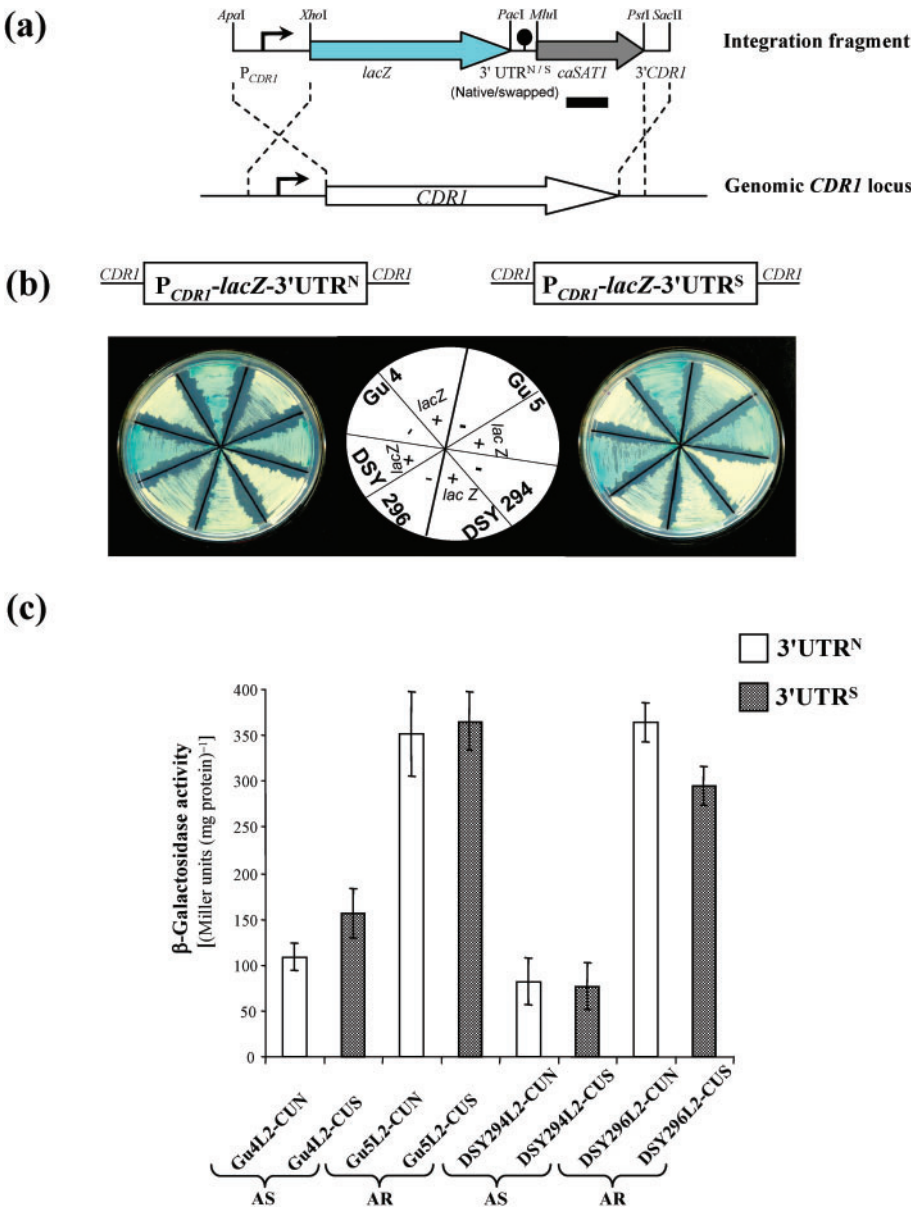

Fig. 3. Schematic depiction of *lacZ* reporter fusion integrants and qualitative and quantitative assay of *β*-galactosidase reporter activity in AS and AR isolates. (a) Structure of the DNA cassettes used to integrate the P_{CDR1}-*lacZ*-3′UTR^N (native) and P_{CDR1}-*lacZ*-3′UTR^S (swapped) reporter fusions into the *CDR1* locus of the clinical *C. albicans* isolates (centre). The *CDR1*- and *lacZ*-coding regions are represented by white and blue arrows, respectively, the *SAT1* marker by a grey arrow, and the 3′ UTR of *CDR1* by the filled circle. *CDR1* upstream and downstream regions are represented by solid lines; the *CDR1* promoter (P_{CDR1}) is symbolized by the bent arrow. The straight arrow indicates the direction of transcription. The probe used to verify the correct integration is indicated by a thick line. Only relevant restriction sites are shown. (b) Transformants harbouring the chromosomally integrated P_{CDR1}-*lacZ*-3′UTR^N (native, left) and P_{CDR1}-*lacZ*-3′UTR^S (swapped, right) constructs and their corresponding parental strains (without *lacZ*) were streaked on minimal medium plates containing X-Gal and photographed after 3 days of growth at 30 °C. The positions of the individual strains on the plates are shown in the scheme (centre). (c) *β*-Galactosidase quantitative reporter activities of each transformant were determined as described in Methods. The reported quantities are mean ± SD (indicated by error bars) of three independent experiments with duplicate measurements of two independent clones. Empty and filled bars indicate P_{CDR1}-*lacZ*-3′UTR^N (native) and P_{CDR1}-*lacZ*-3′UTR^S (swapped) reporter fusion transformants in both AS and AR backgrounds.

Table 1. Representative *CDR1* transcript poly(A) tail lengths and corresponding transcript half-lives in clinical AS and AR isolates

Strain	*CDR1* transcript poly(A) tail length	*CDR1* transcript half-life* [$t_{1/2}$ (min)]
Gu4	26±2	~60
Gu5	35±2	>180
DSY294	24±2	~60
DSY296	36±2	>180

*The *CDR1* transcript half-lives of the mentioned matched pairs of AS and AR isolates were deduced previously (Manoharlal *et al.*, 2008).

detailed in Methods. We observed from PCR amplicon analyses that while *PAP1-a* and *PAP1-α* alleles were generated from both the AS isolates, only the *PAP1-α* allele could be recovered from AR isolates (Fig. 4).

PAP1-a disruption decreases drug susceptibilities of AS isolates

It has been demonstrated earlier that while both the *PAP1* alleles (Δ*pap1-a/PAP1-α* and *PAP1-a/*Δ*pap1-α*) are independently functional in heterozygous deletion mutants, they are collectively essential, since a Δ*pap1-a*/Tet-*PAP1-α* conditional mutant is not viable under Tet-repressing conditions (Jiang *et al.*, 2008). To get an insight into the functional relevance of the observed *PAP1* allelic status in AS and AR clinical isolates, we used *ura3*$^{-}$ mutants DSY3040 (derived from DSY294) and DSY3041 (derived from DSY296) (Coste *et al.*, 2006). For this, heterozygous mutants of *PAP1-a* (Δ*pap1-a/PAP1-α*) and of *PAP1-α* (*PAP1-a/*Δ*pap1-α*) in AS, and a single *PAP1-α* allele

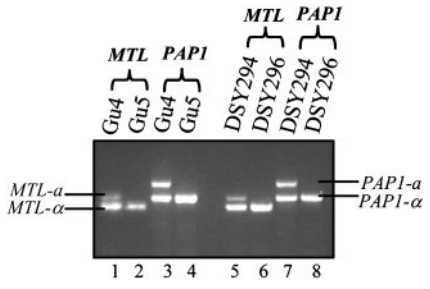

Fig. 4. Analysis of *PAP1* allele status in AS and AR isolates. The *PAP1* allelic status of both the matched clinical pairs was analysed by multiplex PCR using *PAP1-a*- and *PAP1-α*-specific primers (Supplementary Table S1). As a positive control, *MTL* allele-specific primers (*MTL-a* and *MTL-α*) were used. Lanes: 1, Gu4 (*MTL-a/MTL-α*); 2, Gu5 (*MTL-α/MTL-α*); 3, Gu4 (*PAP1-a/PAP1-α*); 4, Gu5 (*PAP1-α/PAP1-α*); 5, DSY294 (*MTL-a/MTL-α*), 6, DSY296 (*MTL-α/MTL-α*); 7, DSY294 (*PAP1-a/PAP1-α*); 8, DSY296 (*PAP1-α/PAP1-α*).

disruptant (Δ*pap1-α/PAP1-α*) in AR, were constructed, as detailed in Methods. These heterozygous *PAP1* mutants were tested for their drug susceptibilities, wherein drug spot assays were performed on YEPD plates containing fixed drug concentrations (Fig. 5a, b). The heterozygous *PAP1-a* mutant (Δ*pap1-a/PAP1-α*) of AS isolates revealed reduced susceptibility to tested drugs as compared with the parental strain DSY3040 (Fig. 5a). Notably, the observed reduced susceptibility of the heterozygous *PAP1-a* mutant (Δ*pap1-a/PAP1-α*) of the AS isolate to the tested drugs could be reversed if complemented with the *PAP1-a* allele (Δ*pap1-a/PAP1-α*+*PAP1-a*). On the other hand, the heterozygous disruption of *PAP1-α* and its complementation in both AS and AR isolates resulted in drug sensitivities comparable with those of the respective parental strains, DSY3040 and DSY3041 (Fig. 5a, b).

PAP1-a disruption (Δ*pap1-a/PAP1-α*) results in hyperadenylation of *CDR1* transcripts in AS isolates

We checked further whether heterozygous disruption of *PAP1-a* and *PAP1-α* in AS and AR isolates could affect the polyadenylation of *CDR1* transcripts. For this, we carried out PAT analysis (as described in Methods) with the heterozygous *PAP1-a* mutant (Δ*pap1-a/PAP1-α*). This analysis revealed that *PAP1-a* deletion in DSY3040 (24±2 A residues) leads to hyperadenylation (35±2 A residues) of *CDR1* transcripts (Table 2). Notably, the complementation of the heterozygous *PAP1-a* mutant with *PAP1-a* (Δ*pap1-a/PAP1-α*+*PAP1-a*) restored the polyadenylation status of *CDR1* transcripts to basal level (Table 2). In contrast, the disruption of *PAP1-α* (*PAP1-a/*Δ*pap1-α*) as well as its subsequent complementation (*PAP1-a/*Δ*pap1-α*+*PAP1-α*) in AS did not affect the polyadenylation of the *CDR1* transcript (Table 2). With regard to the *PAP1-α* allele in the AR isolate, neither its heterozygous disruption (Δ*pap1-α/PAP1-α*) nor its complementation (Δ*pap1-α/PAP1-α*+*PAP1-α*) influenced the polyadenylation status of *CDR1* transcripts (Table 2).

PAP1-a disruption results in increased stability of *CDR1* transcripts in AS isolates

Since, in eukaryotes, most mature mRNAs having a poly(A) tail at their 3′ end participate in mRNA stability (Higgins, 1991; McCarthy, 1998; Ross, 1996), we evaluated whether the observed decrease in drug susceptibility and increase in polyadenylation of *CDR1* transcripts in a heterozygous *PAP1-a* mutant (Δ*pap1-a/PAP1-α*) within the AS background correlates with enhanced stability of its mRNA. Using a thiolutin chase assay, we revealed increased half-life of *CDR1* transcripts ($t_{1/2}$ ~120 min) in a Δ*pap1-a/PAP1-α* mutant (RMY4) in contrast to its parental counterpart, DSY3040 ($t_{1/2}$ ~60 min). The increased *CDR1* transcript stability of RMY4 could be reversed to parental levels if complemented with the *PAP1-a* allele (Δ*pap1-a/PAP1-α*+*PAP1-a*) (Fig. 6a, b). It is of note that the *CDR1* mRNA decay rate of the heterozygous *PAP1-a* mutant

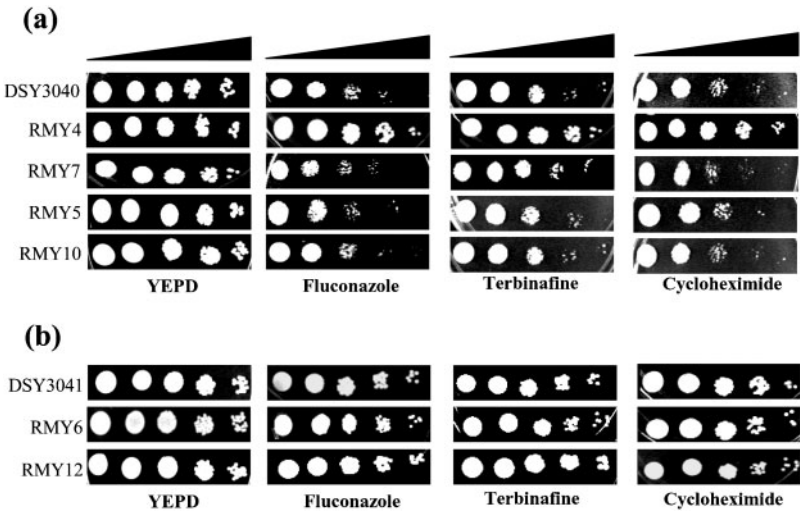

Fig. 5. Drug susceptibility testing of *PAP1* mutants and revertant clinical strains. Drug susceptibility assays were carried out on YEPD medium containing 2 μg fluconazole ml^{-1} (for AS) and 5 μg fluconazole ml^{-1} (for AR), 15 μg terbinafine ml^{-1} and 300 μg cycloheximide ml^{-1}. Spotting assays were performed with serial dilutions of overnight cultures onto YEPD medium containing the indicated drugs. Plates were incubated for 48 h at 30 °C. Graduation filled bars indicate 10-fold serial dilutions of culture, as described in Methods. Strains and genotypes: DSY3040, *PAP1-a/PAP1-α*; RMY4, Δ*pap1-a/PAP1-α*; RMY7, Δ*pap1-a/PAP1-α*+*pap1-a*; RMY5, *PAP1-a/*Δ*pap1-α*; RMY10, *PAP1-a/*Δ*pap1-α*+*PAP1-α*; DSY3041, *PAP1-α/PAP1-α*; RMY6, Δ*pap1-α/PAP1-α*; RMY12, Δ*pap1-α/PAP1-α*+*PAP1-α*.

remained intermediate ($t_{1/2}$ ~120 min) to that of AS ($t_{1/2}$ ~60 min) and AR isolates ($t_{1/2}$ ~180 min) (Fig. 6a, b), indicating that along with *PAP1-α*, some additional unknown mechanism(s) also contribute to enhanced *CDR1* transcript stability in AR isolates. Notably, heterozygous *PAP1-α* mutants of AS (Δ*pap1-a/PAP1-α*) and AR isolates (Δ*pap1-α/PAP1-α*), and their complemented counterparts, *PAP1-a/*Δ*pap1-α*+*PAP1-a* and Δ*pap1-α/PAP1-α*+*PAP1-α*, respectively, did not affect the stability of *CDR1* transcripts (Fig. 6a, b).

DISCUSSION

In many AR clinical isolates of *C. albicans*, a positive correlation between resistance and *CDR1* overexpression has been reported by several independent research groups (Franz *et al.*, 1998, 1999; Lopez-Ribot *et al.*, 1998; White, 1997; White *et al.*, 1998). Various other studies have dissected the *cis*-acting elements in the *CDR1* promoter region (De Micheli *et al.*, 2002; Gaur *et al.*, 2004; Karnani *et al.*, 2004; Puri *et al.*,1999) and identified its transcription factor(s) (Chen *et al.*, 2004; Coste *et al.*, 2006; Znaidi *et al.*, 2008), which contribute to its differential mRNA expression in AS and AR isolates. We have recently observed that along with increased transcriptional activation, enhanced mRNA stability can also contribute to the sustained *CDR1* overexpression in AR isolates (Manoharlal *et al.*, 2008). In the present study, we evaluated the cause(s) of the increased *CDR1* mRNA stability in AR isolates.

Table 2. Representative *CDR1* transcript poly(A) tail lengths and corresponding transcript half-lives in *PAP1* mutant and revertant clinical strains

Strains and genotypes: DSY3040, *PAP1-a/PAP1-α*; RMY4, Δ*pap1-a/PAP1-α*; RMY7, Δ*pap1-a/PAP1-α*+*PAP1-a*; RMY5, *PAP1-a/*Δ*pap1-α*; RMY10, *PAP1-a/*Δ*pap1-α*+*PAP1-α*; DSY3041, *PAP1-α/PAP1-α*; RMY6, Δ*pap1-α/PAP1-α*; RMY12, Δ*pap1-α/PAP1-α*+*PAP1-α*.

Strain	*CDR1* transcript poly(A) tail length	*CDR1* transcript half-life [$t_{1/2}$ (min)]
DSY3040	24±2	~60
RMY4	35±2	~120
RMY7	24±2	~60
RMY5	24±2	~60
RMY10	24±2	~60
DSY3041	36±2	~180
RMY6	36±2	~180
RMY12	36±2	~180

By employing a 3′-RACE method, we mapped and observed the variation in the length of the 3′ UTR of *CDR1* in AS and AR isolates (Fig. 1a, b). Notably, the heterogeneous product lengths at the 3′ ends observed were not specific to AS or AR isolates, since each isolate exhibited a 3′ UTR length for *CDR1* independent of the azole susceptibility as well as of the level of *CDR1* expression. The existence of this heterogeneity at the 3′ end of *CDR1* can be explained by the alternative usage of several polyadenylation signals, as has been well documented for other unrelated *MDR* genes (Edwalds-Gilbert *et al.*, 1997; Hsu *et al.*, 1990). For example, although evolutionarily quite distant from yeast, mouse *mdr1a* (Hsu *et al.*, 1990) and *EhPgp5* mRNA of *Entamoeba histolytica* trophozoites responsible for the MDR phenotype (Lopez-Camarillo *et al.*, 2003) also show length variations at their 3′ ends, which affects mRNA half-life. Notably, several other yeast genes also produce multiple transcripts with different 3′ ends as a result of a carbon source-regulated choice between alternative polyadenylation sites (Sparks & Dieckmann, 1998).

In silico analysis and secondary structure prediction of mapped *CDR1* 3′ UTR (~78 % AU-rich) suggest the

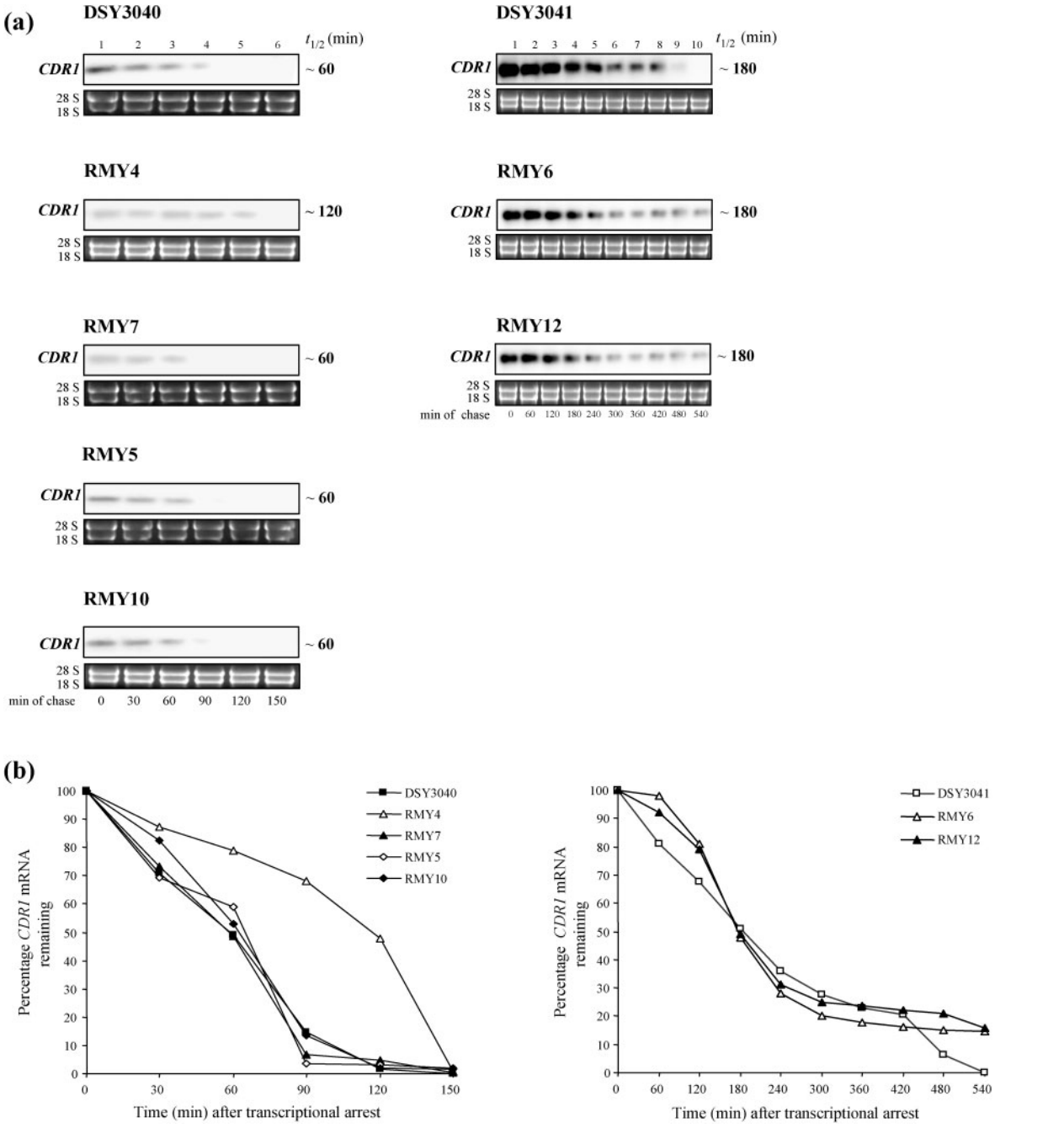

Fig. 6. *CDR1* mRNA decay assay. Exponentially growing cultures of *C. albicans* were incubated with the optimized thiolutin concentration (40 μg ml^{-1}) to inhibit ongoing *in vivo* transcription (as described in Methods). Total RNA was isolated at the times indicated thereafter and fractionated on a 1 % (w/v) agarose/2.2 M formaldehyde denaturing gel. (a) The gel was stained with ethidium bromide before blotting to monitor equal loading of the RNA and subsequently blotted onto a charged nylon membrane. The blot was hybridized with [α-^{32}P]dATP-labelled *CDR1*-specific probe. Time points in minutes are indicated below the equally loaded RNA gel. (b) The hybridization signals were quantified using densitometry scanning in a phosphorimager scanner. The signal intensity at each time point was normalized to that of time t_0 (expressed as a percentage) and plotted as a line graph. $t_{1/2}$, half-life. Strains and genotypes: DSY3040, *PAP1-a/PAP1-α*; RMY4, Δ*pap1-a/PAP1-α*; RMY7, Δ*pap1-a/PAP1-α*+*PAP1-a*; RMY5, *PAP1-a*/Δ*pap1-α*; RMY10, *PAP1-a*/Δ*pap1-α*+*PAP1-α*; DSY3041, *PAP1-α/PAP1-α*; RMY6, Δ*pap1-α/PAP1-α*; RMY12, Δ*pap1-α/PAP1-α*+*PAP1-α*.

existence of various regulatory RNA sequences and structural motifs in both AS and AR isolates (Fig. 2a, b and Supplementary Fig. S1). To experimentally test the proposed mRNA destabilizing activity of these predicted *CDR1* 3′ UTR regulatory motifs, the reporter activity of *lacZ* in transcriptional fusion with the *CDR1* 3′ UTR of either AS or AR isolates was examined (Fig. 3a). Interestingly, swapping of the *CDR1* 3′ UTR between AS and AR had no effect on *lacZ* reporter activities (Fig. 3b, c) or on its mRNA half-life (Supplementary Fig. S2), indirectly indicating that the *CDR1* 3′ UTR is not sufficient to affect either the transcription or the mRNA stability of *CDR1*. Notably, mammalian *MDR1* 3′ UTR (Prokipcak *et al.*, 1999) and *EhPgp5* 3′ UTR (Lopez-Camarillo *et al.*, 2003), which also harbour putative regulatory RNA motifs, do not behave as active destabilizing elements for their corresponding mRNAs.

The mRNA abundance of a typical gene is affected by a concerted interplay of key factors such as the activities of poly(A) polymerase, deadenylases and poly(A)-binding proteins (Zhao *et al.*, 1999). The pre-mRNAs are polyadenylated in a reaction involving 3′-endonucleolytic cleavage followed by poly(A) tail synthesis (Zhao *et al.*, 1999). The poly(A) tail is considered to be a strong modulator of mRNA stability, and its length is subjected to cellular control throughout the life span of the mRNA (Higgins, 1991; McCarthy, 1998; Ross, 1996). It is well known that longer poly(A) tails provide higher stability to mRNA and promote a more efficient translation (Higgins, 1991; McCarthy, 1998; Ross, 1996). In our study, PAT assay revealed that *CDR1* mRNA has an ~30–35 % longer poly(A) tail in AR strains than in their respective matched AS isolates (Table 1), suggesting that polyadenylation and deadenylation events occur at different rates that could affect *CDR1* mRNA half-life. The relatively longer poly(A) tail of *EhPgp5* mRNA has been shown to be associated with its enhanced half-life in *Entamoeba histolytica* trophozoites grown in the presence of the drug emetine (Lopez-Camarillo *et al.*, 2003). Interestingly, this increased poly(A) tail length of *EhPgp5* mRNA has been associated with the *Entamoeba histolytica* nuclear poly(A) polymerase (*EhPAP*) that catalyses the poly(A) tail synthesis of mRNA in the nucleus (Garcia-Vivas *et al.*, 2005).

C. albicans PAP1, which is responsible for polyadenylation of mRNA, is located within the *MTL* locus on chromosome 5, where *TAC1* and its linkage with the *MTL* in determining *TAC1* hyperactivity have been established (Coste *et al.*, 2006). It has been recently shown that a hyperactive *TAC1* allele is responsible for *CDR1* as well as *CDR2* upregulation in isolate DSY296 (Coste *et al.*, 2006). The existence of an association among *MTL*, *TAC1* and *PAP1* is an exciting possibility that needs to be explored. It is of note that Sanglard's group has shown by comparative genome hybridization (CGH) and single nucleotide polymorphism (SNP) arrays that LOH of *TAC1* in an AR clinical isolate (DSY296) can occur either by recombination between portions of chromosome 5 or by chromosome 5 duplication. LOH is not restricted to *MTL* but also extends to ~250 kb flanking regions that also comprise *PAP1* alleles within *MTL* (Coste *et al.*, 2006). Consistent with published results, we recovered two distinct *PAP1* alleles (*PAP1-a*/*PAP1-*α) from AS (*MTL-a*/*MTL-*α) and a single type of *PAP1* allele (*PAP1-*α) in matched AR isolates (*MTL-*α/*MTL-*α) (Fig. 4). It is of note that these two isoforms of *C. albicans PAP1*, *PAP1-a* (ORF 19.3197) and *PAP1-*α (ORF 19.10713), share only ~70 % amino acid identity (Hull & Johnson, 1999). Earlier evidence of differential susceptibilities of the two *PAP1* isoforms to a natural product, parnafungin, suggests a difference in their *in vivo* activity (Jiang *et al.*, 2008). We established differences in *PAP1-a* and *PAP1-*α activities by constructing heterozygous mutants in both AS and AR backgrounds. Notably, the heterozygous *PAP1-a* mutant (Δ*pap1-a/PAP1-*α) displayed enhanced drug resistance as compared with the AS isolate (Fig. 5a), which could be reversed by complementing the *PAP1-a* allele in this heterozygous mutant (Δ*pap1-a/PAP1-*α + *PAP1-a*, Fig. 5a). Subsequent analysis of relative hyperadenylation (Table 2) and decreased decay rate of *CDR1* mRNA (Fig. 6a, b) in this heterozygous *PAP1-a* mutant suggests that *PAP1-a* has a dominant negative effect on *PAP1-*α activity. It seems that *PAP1-a* disruption in AS isolates leads to de-repression of *PAP1-*α activity, thereby leading to hyperadenylation and increased stability of *CDR1* transcripts. This observation is consistent with the unchanged drug susceptibilities of heterozygous *PAP1-*α mutant in both AS (*PAP1-a/*Δ*pap1-*α) and AR (Δ*pap1-*α*/PAP1-*α) isolates (Fig. 5a, b). This was accompanied by unaltered polyadenylation status (Table 2) as well as stability of *CDR1* transcripts (Fig. 6a, b). However, it should be noted that in the heterozygous *PAP1-a* mutant of AS isolates, although *CDR1* transcript polyadenylation status switches from AS to AR level (24 ± 2 to 35 ± 2 A residues), its mRNA decay rate remains intermediate ($t_{1/2}$ ~120 min) to that of AS ($t_{1/2}$ ~60 min) and AR isolates ($t_{1/2}$ ~180 min) (Fig. 6a, b, Table 2). This implies that along with increased poly(A) tail length, some additional mechanism(s) also contribute to enhanced *CDR1* transcript stability in AR isolates.

In conclusion, our results provide what we believe to be the first evidence that LOH at the *PAP1* locus contributes to hyperadenylation and subsequent increased *CDR1* transcript stability, and ultimately enhanced drug resistance in AR isolates. We recently observed that all *TAC1* target genes show relatively higher transcriptional rates and mRNA half-lives in AR isolates (our unpublished observations). However, whether the observed increase in poly(A) tail length in AR isolates is specific to *CDR1* transcripts alone or represents a general feature of the mRNA population of Tac1p targets as well as other transcripts within the ORFome of *C. albicans* remains to be established. Certainly, further characterization of the functional role of *PAP1* should lead to a better understanding of mechanisms underlying post-transcriptional events and should also be useful for the development of

antifungal strategies that can be exploited to combat MDR in *C. albicans*.

ACKNOWLEDGEMENTS

We are grateful to Joachim Morschhäuser, Universität Würzburg, Germany, for providing the clinical isolates Gu4/Gu5. We thank Chinmay K. Mukhopadhyay, Special Centre for Molecular Medicine (SCMM), Jawaharlal Nehru University, New Delhi, India, for providing the valuable advice on the PAT assay. Thiolutin (CP-4092) and fluconazole were provided as generous gifts from Pfizer and Ranbaxy Laboratories, respectively. The work presented in this paper has been supported in part by grants to R. P. from the Department of Science and Technology, Indo-Swiss (INT/SWISS/P-31/2009), Department of Biotechnology (BT/PR9100/Med/29/ 03/2007, BT/PR9563/BRB/10/ 567/2007, BT/PR11158/BRB/10/640/2008) and the Council of Scientific and Industrial Research (CSIR) [38(1122)/06/EMR-II]. R. M. thanks CSIR for the award of a senior research fellowship.

REFERENCES

Akins, R. A. (2005). An update on antifungal targets and mechanisms of resistance in *Candida albicans*. *Med Mycol* **43**, 285–318.

Chen, C. G., Yang, Y. L., Shih, H. I., Su, C. L. & Lo, H. J. (2004). *CaNdt80* is involved in drug resistance in *Candida albicans* by regulating *CDR1*. *Antimicrob Agents Chemother* **48**, 4505–4512.

Coste, A. T., Karababa, M., Ischer, F., Bille, J. & Sanglard, D. (2004). *TAC1*, transcriptional activator of *CDR* genes, is a new transcription factor involved in the regulation of *Candida albicans* ABC transporters *CDR1* and *CDR2*. *Eukaryot Cell* **3**, 1639–1652.

Coste, A., Turner, V., Ischer, F., Morschhäuser, J., Forche, A., Selmecki, A., Berman, J., Bille, J. & Sanglard, D. (2006). A mutation in Tac1p, a transcription factor regulating *CDR1* and *CDR2*, is coupled with loss of heterozygosity at chromosome 5 to mediate antifungal resistance in *Candida albicans*. *Genetics* **172**, 2139–2156.

De Micheli, M., Bille, J., Schuller, C. & Sanglard, D. (2002). A common drug-responsive element mediates the upregulation of the *Candida albicans* ABC transporters *CDR1* and *CDR2*, two genes involved in antifungal drug resistance. *Mol Microbiol* **43**, 1197–1214.

Edwalds-Gilbert, G., Veraldi, K. L. & Milcarek, C. (1997). Alternative poly(A) site selection in complex transcription units: means to an end? *Nucleic Acids Res* **25**, 2547–2561.

Fonzi, W. A. & Irwin, M. Y. (1993). Isogenic strain construction and gene mapping in *Candida albicans*. *Genetics* **134**, 717–728.

Franz, R., Kelly, S. L., Lamb, D. C., Kelly, D. E., Ruhnke, M. & Morschhäuser, J. (1998). Multiple molecular mechanisms contribute to a stepwise development of fluconazole resistance in clinical *Candida albicans* strains. *Antimicrob Agents Chemother* **42**, 3065–3072.

Franz, R., Ruhnke, M. & Morschhäuser, J. (1999). Molecular aspects of fluconazole resistance development in *Candida albicans*. *Mycoses* **42**, 453–458.

Garcia-Vivas, J., Lopez-Camarillo, C., Zuara-Liceaga, E., Orozco, E. & Marchat, L. A. (2005). *Entamoeba histolytica*: cloning and expression of the poly(A) polymerase *EhPAP*. *Exp Parasitol* **110**, 226–232.

Gaur, N. A., Puri, N., Karnani, N., Mukhopadhyay, G., Goswami, S. K. & Prasad, R. (2004). Identification of a negative regulatory element which regulates basal transcription of a multidrug resistance gene *CDR1* of *Candida albicans*. *FEMS Yeast Res* **4**, 389–399.

Gerads, M. & Ernst, J. F. (1998). Overlapping coding regions and trancriptional units of two essential chromosomal genes (*CCT8*, *TRP1*) in the fungal pathogen *Candida albicans*. *Nucleic Acids Res* **26**, 5061–5066.

Higgins, C. F. (1991). Stability and degradation of mRNA. *Curr Opin Cell Biol* **3**, 1013–1018.

Holm, L. & Sander, C. (1995). DNA polymerase β belongs to ancient nucleotidyltransferase superfamily. *Trends Biochem Sci* **20**, 345–347.

Hsu, S. I., Cohen, D., Kirschner, L. S., Lothstein, L., Hartstein, M. & Horwitz, S. B. (1990). Structural analysis of the mouse *mdr1a* (P-glycoprotein) promoter reveals the basis for differential transcript heterogeneity in multidrug-resistant J774.2 cells. *Mol Cell Biol* **10**, 3596–3606.

Hull, C. M. & Johnson, A. D. (1999). Identification of a mating type-like locus in the asexual pathogenic yeast *Candida albicans*. *Science* **285**, 1271–1275.

Jiang, B., Xu, D., Allocco, J., Parish, C., Davison, J., Veillette, K., Sillaots, S., Hu, W., Rodriguez-Suarez, R. & other authors (2008). PAP inhibitor with in vivo efficacy identified by *Candida albicans* genetic profiling of natural products. *Chem Biol* **15**, 363–374.

Karnani, N., Gaur, N. A., Jha, S., Puri, N., Krishnamurthy, S., Goswami, S. K., Mukhopadhyay, G. & Prasad, R. (2004). SRE1 and SRE2 are two specific steroid-responsive modules of *Candida* drug resistance gene 1 (*CDR1*) promoter. *Yeast* **21**, 219–239.

Kusov, Y. Y., Shatirishvili, G., Dzagurov, G. & Gauss-Muller, V. (2001). A new G-tailing method for the determination of the poly(A) tail length applied to hepatitis A virus RNA. *Nucleic Acids Res* **29**, E57.

Lopez-Camarillo, C., Luna-Arias, J. P., Marchat, L. A. & Orozco, E. (2003). *EhPgp5* mRNA stability is a regulatory event in the *Entamoeba histolytica* multidrug resistance phenotype. *J Biol Chem* **278**, 11273–11280.

Lopez-Ribot, J. L., McAtee, R. K., Lee, L. N., Kirkpatrick, W. R., White, T. C., Sanglard, D. & Patterson, T. F. (1998). Distinct patterns of gene expression associated with development of fluconazole resistance in serial *Candida albicans* isolates from human immunodeficiency virus-infected patients with oropharyngeal candidiasis. *Antimicrob Agents Chemother* **42**, 2932–2937.

Magee, B. B. & Magee, P. T. (2000). Induction of mating in *Candida albicans* by construction of *MTLa* and *MTL*α strains. *Science* **289**, 310–313.

Manoharlal, R., Gaur, N. A., Panwar, S. L., Morschhäuser, J. & Prasad, R. (2008). Transcriptional activation and increased mRNA stability contribute to overexpression of *CDR1* in azole-resistant *Candida albicans*. *Antimicrob Agents Chemother* **52**, 1481–1492.

McCarthy, J. E. (1998). Post-transcriptional control of gene expression in yeast. *Microbiol Mol Biol Rev* **62**, 1492–1553.

Morschhäuser, J., Barker, K. S., Liu, T. T., Blaß-Warmuth, J., Homayouni, R. & Rogers, P. D. (2007). The transcription factor Mrr1p controls expression of the *MDR1* efflux pump and mediates multidrug resistance in *Candida albicans*. *PLoS Pathog* **3**, e164.

Murad, A. M., Lee, P. R., Broadbent, I. D., Barelle, C. J. & Brown, A. J. (2000). CIp10, an efficient and convenient integrating vector for *Candida albicans*. *Yeast* **16**, 325–327.

Pesole, G. & Liuni, S. (1999). Internet resources for the functional analysis of 5′ and 3′ untranslated regions of eukaryotic mRNAs. *Trends Genet* **15**, 378.

Pesole, G., Liuni, S., Grillo, G., Licciulli, F., Mignone, F., Gissi, C. & Saccone, C. (2002). UTRdb and UTRsite: specialized databases of sequences and functional elements of 5′ and 3′ untranslated regions of eukaryotic mRNAs. Update. *Nucleic Acids Res* **30**, 335–340.

Prasad, R., De, W. P., Goffeau, A. & Balzi, E. (1995). Molecular cloning and characterization of a novel gene of *Candida albicans*,

CDR1, conferring multiple resistance to drugs and antifungals. *Curr Genet* **27**, 320–329.

Prokipcak, R. D., Raouf, A. & Lee, C. (1999). The AU-rich 3′ untranslated region of human *MDR1* mRNA is an inefficient mRNA destabilizer. *Biochem Biophys Res Commun* **261**, 627–634.

Puri, N., Krishnamurthy, S., Habib, S., Hasnain, S. E., Goswami, S. K. & Prasad, R. (1999). *CDR1*, a multidrug resistance gene from *Candida albicans*, contains multiple regulatory domains in its promoter and the distal AP-1 element mediates its induction by miconazole. *FEMS Microbiol Lett* **180**, 213–219.

Reuss, O., Vik, A., Kolter, R. & Morschhäuser, J. (2004). The *SAT1* flipper, an optimized tool for gene disruption in *Candida albicans*. *Gene* **341**, 119–127.

Rognon, B., Kozovska, Z., Coste, A. T., Pardini, G. & Sanglard, D. (2006). Identification of promoter elements responsible for the regulation of *MDR1* from *Candida albicans*, a major facilitator transporter involved in azole resistance. *Microbiology* **152**, 3701–3722.

Ross, J. (1996). Control of messenger RNA stability in higher eukaryotes. *Trends Genet* **12**, 171–175.

Russell, J. E., Morales, J., Makeyev, A. V. & Liebhaber, S. A. (1998). Sequence divergence in the 3′ untranslated regions of human ζ- and α-globin mRNAs mediates a difference in their stabilities and contributes to efficient α- to -ζ gene development switching. *Mol Cell Biol* **18**, 2173–2183.

Sanglard, D. & Odds, F. C. (2002). Resistance of *Candida* species to antifungal agents: molecular mechanisms and clinical consequences. *Lancet Infect Dis* **2**, 73–85.

Sanglard, D., Kuchler, K., Ischer, F., Pagani, J. L., Monod, M. & Bille, J. (1995). Mechanisms of resistance to azole antifungal agents in *Candida albicans* isolates from AIDS patients involve specific multidrug transporters. *Antimicrob Agents Chemother* **39**, 2378–2386.

Sanglard, D., Ischer, F., Monod, M. & Bille, J. (1996). Susceptibilities of *Candida albicans* multidrug transporter mutants to various antifungal agents and other metabolic inhibitors. *Antimicrob Agents Chemother* **40**, 2300–2305.

Sanglard, D., Ischer, F., Monod, M. & Bille, J. (1997). Cloning of *Candida albicans* genes conferring resistance to azole antifungal agents: characterisation of *CDR2*, a new multidrug ABC transporter gene. *Microbiology* **143**, 405–416.

Sparks, K. A. & Dieckmann, C. L. (1998). Regulation of poly(A) site choice of several yeast mRNAs. *Nucleic Acids Res* **26**, 4676–4687.

Talibi, D. & Raymond, M. (1999). Isolation of a putative *Candida albicans* transcriptional regulator involved in pleiotropic drug resistance by functional complementation of a *pdr1 pdr3* mutation in *Saccharomyces cerevisiae*. *J Bacteriol* **181**, 231–240.

Thompson, J. D., Higgins, D. G. & Gibson, T. J. (1994). CLUSTAL W: improving the sensitivity of progressive multiple sequence alignment through sequence weighting, position-specific gap penalties and weight matrix choice. *Nucleic Acids Res* **22**, 4673–4680.

Trzaska, D. & Dastych, J. (2005). Role of AURE sequences in the regulation of mRNA stability. *Postepy Biochem* **51**, 28–35.

Uhl, M. A. & Johnson, A. D. (2001). Development of *Streptococcus thermophilus lacZ* as a reporter gene for *Candida albicans*. *Microbiology* **147**, 1189–1195.

White, T. C. (1997). Increased mRNA levels of *ERG16*, *CDR*, and *MDR1* correlate with increases in azole resistance in *Candida albicans* isolates from a patient infected with human immunodeficiency virus. *Antimicrob Agents Chemother* **41**, 1482–1487.

White, T. C., Pfaller, M. A., Rinaldi, M. G., Smith, J. & Redding, S. W. (1997). Stable azole drug resistance associated with a substrain of *Candida albicans* from an HIV-infected patient. *Oral Dis* **3** (suppl. 1), S102–S109.

White, T. C., Marr, K. A. & Bowden, R. A. (1998). Clinical, cellular, and molecular factors that contribute to antifungal drug resistance. *Clin Microbiol Rev* **11**, 382–402.

Wirsching, S., Michel, S., Kohler, G. & Morschhäuser, J. (2000). Activation of the multiple drug resistance gene *MDR1* in fluconazole-resistant, clinical *Candida albicans* strains is caused by mutations in a *trans*-regulatory factor. *J Bacteriol* **182**, 400–404.

Yang, Y. L., Lin, Y. H., Tsao, M. Y., Chen, C. G., Shih, H. I., Fan, J. C., Wang, J. S. & Lo, H. J. (2006). Serum repressing efflux pump *CDR1* in *Candida albicans*. *BMC Mol Biol* **7**, 22.

Zhao, J., Hyman, L. & Moore, C. (1999). Formation of mRNA 3′ ends in eukaryotes: mechanism, regulation, and interrelationships with other steps in mRNA synthesis. *Microbiol Mol Biol Rev* **63**, 405–445.

Znaidi, S., Weber, S., Zin Al-Abdin, O., Bomme, P., Saidane, S., Drouin, S., Lemieux, S., De, D. X., Robert, F. & Raymond, M. (2008). Genome-wide location analysis of *Candida albicans* Upc2p, a regulator of sterol metabolism and azole drug resistance. *Eukaryot Cell* **7**, 836–847.

Zuker, M., Mathews, D. H. & Turner, D. H. (1999). Algorithms and thermodynamics for RNA secondary structure prediction: a practical guide. In *RNA Biochemistry and Biotechnology*, pp. 11–43. Edited by J. Barciszewski & B. F. C. Clark. Boston, MA: Kluwer Academic Publishers.

Edited by: J. F. Ernst